THE ASTROPHYSICAL JOURNAL, 418:850–854, 1993 December 1

ULTRAVIOLET MORPHOLOGIES OF GLOBULAR CLUSTERS OBSERVED WITH THE ULTRAVIOLET IMAGING TELESCOPE

ERIC P. SMITH,[1,2] WAYNE B. LANDSMAN,[3] ROBERT S. HILL,[3] RALPH C. BOHLIN,[4] KWANG-PING CHENG,[2,5] PAUL HINTZEN,[1,2,6] STEPHEN P. MARAN,[1] ROBERT W. O'CONNELL,[7] MORTON S. ROBERTS,[8] ANDREW M. SMITH,[1] AND THEODORE P. STECHER[1]

Received 1992 December 31; accepted 1993 June 8

ABSTRACT

We compare the ultraviolet (UV) and visible morphologies of globular clusters M3, M13, M79, and ω Cen, based on observations with the Ultraviolet Imaging Telescope (UIT) and ground-based telescopes. Global similarities (e.g., core radii) are found, along with other interesting features. These include a ring ($r = 2'.2$) of UV-bright stars in ω Cen and a group of UV-bright objects near the center of M79. We find a color gradient in M79 but in no other cluster. The helium abundance in M79 is $Y = 0.21 \pm 0.04$, based on UV and visible color-magnitude diagrams.

Subject headings: globular clusters: general — stars: horizontal-branch — ultraviolet: stars

1. INTRODUCTION

Ultraviolet (UV) observations of globular cluster morphologies may be used to address questions about cluster evolution and formation conditions. Ironically, such observations are particularly valuable because of their insensitivity to the bulk of the cluster light (e.g., red giants). The mid- and far-UV ($\lambda < 2000$ Å) are natural regions for evolution studies because they are more sensitive to blue horizontal-branch (HB) stars and less affected by the cooler red giants (RGB) and the remaining low-mass main-sequence stars. This sensitivity makes UV observations ideal for searching for color gradients and for measuring the ratio of HB to RGB stars ($R \equiv \mathcal{N}_{HB}/\mathcal{N}_{RG}$). Previous studies of color gradients in globular clusters relied upon difficult measurements of color changes in broad-band, ground based photometry (e.g., Bailyn et al. 1989; Djorgovski, Piotto, & King 1989; Cederbloom et al. 1992). Theoretical interpretations of these color gradients ascribe them to a variation of $\mathcal{N}_{HB}/\mathcal{N}_{RG}$ with radius, with either the HB stars more concentrated toward the center, a centrally enhanced population of blue subdwarfs (see, e.g., Bailyn et al. 1989; Cederbloom et al. 1992), or a central deficit of RGB stars (Djorgovski et al. 1991). A comparison of globular cluster UV and visible light radial profiles should be maximally sensitive to any color gradient.

A common way of measuring the He abundance in globular clusters is to compare the relative numbers of HB to RGB stars. This ratio measures the relative lifetimes of these stages and is related to the cluster He abundance (Iben 1968). Typically, the ratios are measured in a small area outside the core radius. The Ultraviolet Imaging Telescope (UIT) data allow us to survey almost the entire cluster to enumerate the blue end of the HB and therefore obtain a global estimate of the value of R.

2. DATA ACQUISITION AND ANALYSIS

2.1. *UIT Mission*

Stecher et al. (1992) describe the UIT instrumentation and initial data reduction. We selected the best exposures of four globular cluster (ω Cen, M3, M13, and M79) in the A1 ($\lambda_0 = 249$ nm, $\Delta\lambda = 115$ nm), A5 ($\lambda_0 = 256$ nm, $\Delta\lambda = 46$ nm), B1 ($\lambda_0 = 152$ nm, $\Delta\lambda = 35$ nm) and B5 ($\lambda_0 = 160$ nm, $\Delta\lambda = 23$ nm) filters for this study. The images have a typical point-spread function (PSF) with a core of FWHM $\sim 3''.5$ and broad wings (80% encircled energy radius = $8''.4$). Except for ω Cen, each cluster was entirely within the $40''$ diameter field. The central $r \sim 13'$ region of ω Cen is well recorded. The exposures on M3 and M13 were shallow, so the outer portions of these clusters were not recorded. Complementary ground-based images (seeing $1''.5$–$2''.0$ FWHM) in U, B, V, and R were obtained with the KPNO and CTIO 0.9 m telescopes and T2KA (KPNO) or TeK2048 (CTIO) CCDs. These visible data were bias-subtracted and flatfielded using sky exposures with standard IRAF[9] software.

2.2. *Data Analysis*

To obtain radial profiles in Figure 1 we made counts in the exterior regions where individual stars are well separated and performed surface photometry of the inner regions where the star images are blended. We derived the backgrounds for surface photometry by computing the mean for several thousand points per frame. No background corrections were applied to the star counts because at UV wavelengths only globular members are likely to have been recorded on the film. (Very bright stars [e.g. UIT-1 and UIT-2; Landsman et al.

[1] Laboratory for Astronomy and Solar Physics, NASA/Goddard Space Flight Center, Code 681, Greenbelt, MD 20771.
[2] Guest observer at the Kitt Peak National Observatory and Cerro Tololo Inter-American Observatory, NOAO, operated by AURA, Inc., under contract to the NSF.
[3] Hughes STX Corporation, Code 681, NASA/Goddard Space Flight Center, Greenbelt, MD 20771.
[4] Space Telescope Science Institute, 3700 San Martin Drive, Baltimore, MD 21218.
[5] National Research Council Postdoctoral Fellow.
[6] Department of Physics and Astronomy, California State University, Long Beach, 1250 Bellflower Avenue, Long Beach, CA 90840.
[7] Astronomy Department, University of Virginia, Charlottesville, VA 22903.
[8] National Radio Astronomy Observatory, Edgemont Road, Charlottesville, VA 22903.

[9] IRAF is distributed by the National Optical Astronomy Observatories, which is operated by the Association of Universities for Research in Astronomy, Inc. (AURA), under cooperative agreement with the National Science Foundation.

1992] are rare and minimally affect star counts.) We used a modified form of DAOPHOT for star counts and the octant method (see Djorgovski et al. 1987) for the surface photometry. Data from the two methods are distinguished in Figure 1. To assure that the two methods gave consistent results, we also did surface photometry at large radii where star counts were made with DAOPHOT, to match the profiles. To determine the cluster centers, we used the mirror autocorrelation technique (Djorgovski 1987), the maximum symmetry method (Hertz & Grindlay 1985) and the equibarycenter (Bijaoui 1971). The centers derived by the various methods agreed within 1 UIT PSF for all but ω Cen. We used the equibarycenter for ω Cen because it is well resolved. After deriving a projected stellar density profile, we made a least-squares fit to the analytic approximation of a King profile:

$$\sigma(r) = \sigma_0\{[1 + (r/r_c)^\alpha]^{-1/2} - [1 + (r_t/r_c)^\alpha]^{-1/2}\}^2$$

(King 1962), where r_c and r_t are the core and tidal radii, respectively, σ_0 is a function of the central surface density, and α is an exponent governing primarily the slope of the outer portion of the profile (for $\alpha = 2$ the profile is a classical "King model"). In practice, r_t was held fixed at a value from Webbink (1985). Because r_t is largely determined by the Galactic tidal field, it should be identical for all stars in the cluster, if the stars whose light dominates in the UV are drawn from the same velocity phase space as the rest of the cluster. We also generated King models via the methods outlined in King (1966) to compare with the UV data.

3. DISCUSSION

3.1. ω *Centauri* (*NGC 5139*)

Figure 1 shows the stellar surface density and surface brightness profiles in the B5 filter for ω Cen, as well as a magnitude-shifted *B* profile from Meylan (1987). The two UV bright stars, UIT-1 and UIT-2 (Landsman et al. 1992), were excised from the data when constructing the profiles. Since ω Cen is relatively close ($d \approx 5.2$ kpc) and loosely concentrated, UIT resolved individual stars into the cluster center (see Landsman et al. 1992, Figs. 2 and 3). On the UIT images, ω Cen appears to have a rather uniform surface density inside $r = 2'$. Figure 1 shows that the B5 profile tracks the *B* profile well, except for the rise in density inside $r = 15''$ and an apparent surface brightness "shoulder" in the profile $r = 2''$. These two features result from the discrete nature of UV-bright stellar distribu-

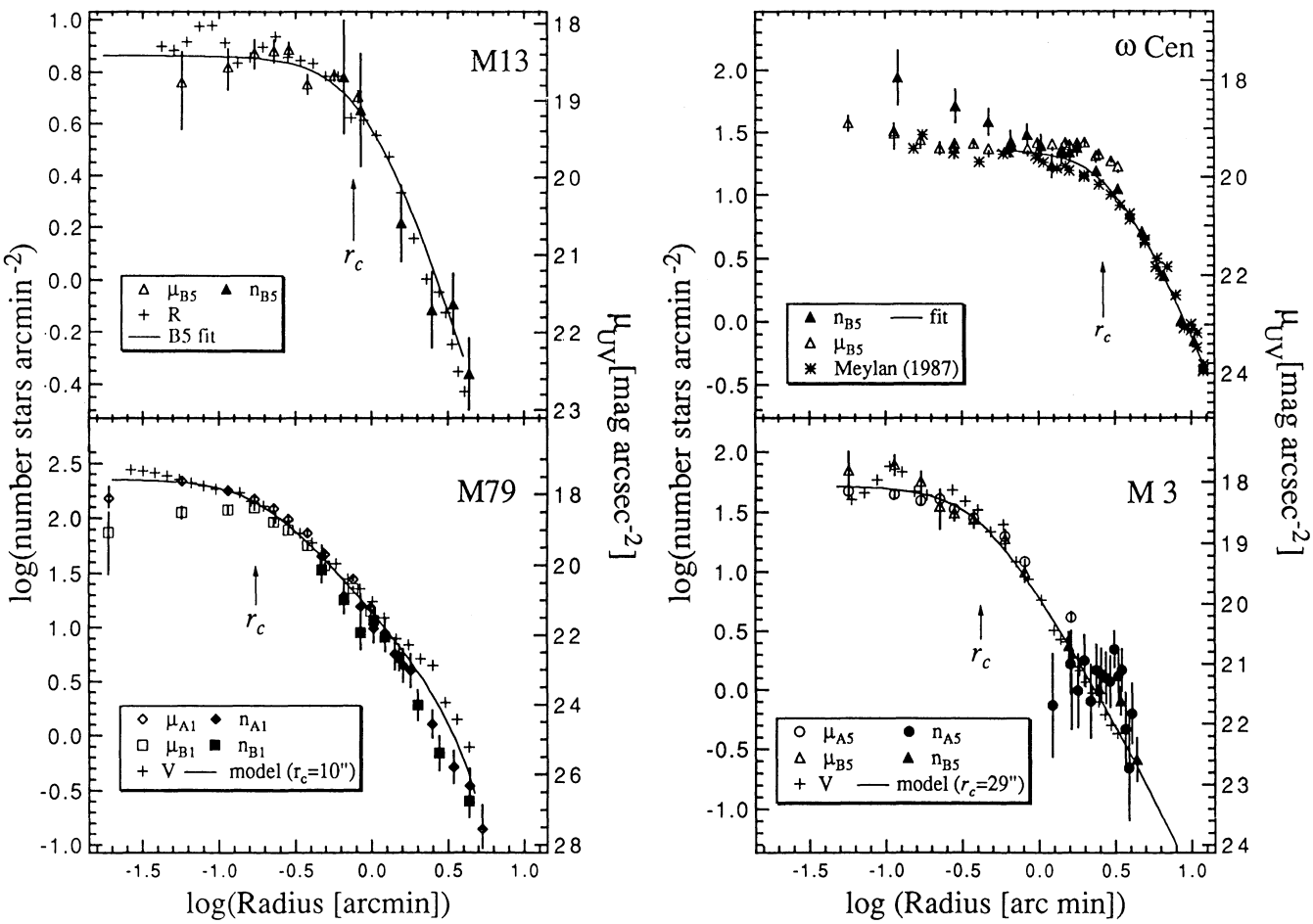

FIG. 1.—Surface density and surface photometry profiles for the four globular clusters. Points derived from star counts (*n*) are plotted as filled symbols, while surface photometry (μ) points are open symbols. Our ground-based data are plotted as plus signs for all bands and specified in each plot. Data from Meylan (1987) are plotted as asterisks. Triangles (*circles*) indicate B5 (A5) data. The A1 data are represented by diamonds and the B1 data by squares. Solid lines show the King model fits. Error bars for the star counts are estimated from Poisson counting statistics. Error bars for the surface photometry represent the standard deviation of the mean for the octants added in quadrature with the standard deviation of the mean background. Core radii for each of the clusters from Webbink (1985) are also plotted in each panel.

tions near the center and an apparent ring of bright stars at $r \sim 2.2'$. The inner peak, arising primarily from the two innermost density points, contains 15 stars very near the cluster center, $\alpha = 13^h26^m45.^s68$, $\delta = -47°28'39.''14$ (2000). If we allow the derived center to vary by $\pm 10''$, this central peak persists. Ground-based images in good seeing (I. R. King 1991, private communication) also suggests a central density peak. Figure 2 shows the radial variation of the mean and median stellar B5 magnitudes, again with stars UIT-1 and UIT-2 (Landsman et al. 1992) removed. Near $r = 2.'2$ there is a large, significant difference between the mean and median magnitudes (~ 0.4 mag) that reflects the presence of a dozen or so UV-bright stars near this radius. This ring, in part, accounts for Scaria & Bappu (1981) finding ω Cen bluer between 2′ and 4′ than elsewhere. Near the image center, the discrete stars and stellar groups produce apparent holes in the UV light distribution. These holes and complementary star knots lead to the peak inside $r = 30''$ (Fig. 1). For the surface brightness to stay constant while the stellar density rises, the mean luminosity of the stars must decrease. We compared magnitudes of stars in different radial annuli to explore this effect and find that inside $r = 30''$ the mean magnitude (prior to extinction corrections) and the rms scatter about the mean are $\langle m_{r<30''} \rangle = 16.58 \pm 0.50$ ($N = 21$ stars). For stars with $2.'5 < r < 10'$ (excludes $r = 2.'2$ ring of bright stars and UV bright stars found by Landsman et al. 1992 and extends to radius of Fig. 1 profile), we find that the mean magnitude is $\langle m_{2.5'<r<10'} \rangle = 16.15 \pm 0.77$ ($N = 892$ stars). This difference is significant at better than the 99% confidence level and suggests that there may be fainter stars near the center. The ω Cen image was reasonably well centered in the UIT field, so that sensitivity losses near the frame edge will not affect the detectability of faint stars in the outer portions of the cluster. We also note that $\langle m_{45''<r<1.5'} \rangle = 16.29 \pm 0.64$ ($N = 105$ stars), which indicates that the observed inner-outer magnitude difference is not solely the consequence of increased sensitivity to faint stars near the cluster center due to the higher background from unresolved cluster members (as might be expected from nonlinearity in the film response at low light levels). ω Cen has a rather large spread in HB magnitude, so that any faint central stars may merely represent the tail end of this distribution. The presence of fainter stars, if confirmed, could imply mass segregation at the center of ω Cen. Bailyn et al. (1992) suggested that the relative number of hot subdwarfs (the so-called subdrawf B stars) increases toward the center of ω Cen. Analysis of the ω Cen color-magnitude (C-M) diagram by Whitney et al. (1993) should indicate whether these fainter stars are indeed hotter, confirming their status as subdwarf B stars.

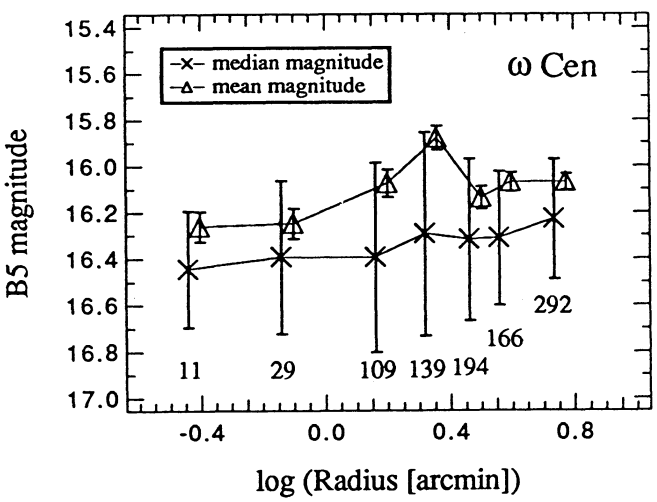

FIG. 2.—Variation of the mean and median B5 magnitude with radius for stars in ω Cen. Points for the mean (median) magnitude have been shifted by 0.02 (−0.2) in log radius for clarity. Error bars for mean magnitudes represent the standard error of the mean, while those for median magnitudes represent the quartile deviations. Fifty percent of all stars within each radial bin have magnitudes within the quartile deviations. Below each set of points we list the number of stars contained in that radial bin.

3.2. *M79 (NGC 1904)*

The UIT obtained useful data on M79 in the A1, B1, and B5 filters. Figure 1 shows the A1, B1, and V profiles, with the V data shifted to overlap the A1 profile, and a King model based on earlier optical observations (Webbink 1985). The central regions are crowded in the UIT images, so surface photometry was used to determine the profiles for $r < 30''$. The A1 and V-band profiles are similar, although there may be some steepening of the UV star counts outside $r = 2.'2$; the errors are large at these radii. The B1 also profile also departs from a King profile shape at small radii. The cluster center for M79 was first determined from a short, unsaturated A1 image as $\alpha = 5^h24^m11.^s17$, $\delta = -24°31'30.''9$ (2000). The stellar distribution, like that of ω Cen, is quite lumpy, with knots of UV bright stars and regions of apparent UV flux deficits. One such UV-dark region, which produces the dip in the B1 profile near $\log r = -1.3$, is centered at $\alpha = 5^h24^m11.^s46$, $\delta = -24°31'25''$ and has a radius of $\sim 10''$. We verified this local UV light minimum by comparing its position in the long (1116 s) B1 exposure to the same regions in shorter exposures in the B1 filter (to check for saturation effects) and the B5 image (Fig. 3 [Pl. 15]). To match the shapes of the B1 and A1 luminosity profiles near the cluster center, ~ 10 stars of the M79 mean HB luminosity would be needed. There are two obvious explanations of the flux deficit in this region: (1) the ratio of red giants and main sequence stars to HB stars is higher, so that there are fewer HB stars per unit volume, or (2) light from HB stars is obscured. Given the close agreement in shape of the inner portions of the ground-based and A1 profiles, the second explanation is not plausible. If there were an extinction enhancement in a small region near the cluster center, there should be a dip in A1 profile relative to the V profile because the A1 filter response is several times more sensitive to dust. Aurière & Leroy (1990) searched for such dark patches in globular clusters without success. It is more likely that the dark patch results from a *local* fluctuation of the relative number densities of HB and RG stars. Regardless of this "dark" patch, which reddens (by ~ 0.7 mag) the central $\sim 10''$ relative to its surroundings, there is a *global* bluing of the cluster with decreasing radius. Using the octant method profiles for the B1 and V data, we determine the color change interior to $r = 4'$ to be $\Delta(B1 - V)/\Delta \log r \cong -0.22$ (Fig. 4). Note several peaks in Figure 3, interior to the region where individual stars are blended. Several of these objects (possibly supra-HB stars or groups of stars) were also seen by Altner & Matilsky (1992) and are partially responsible for the observed color gradient. However, these supra-HB objects cannot account for the entire color gradient, because it is observed over an area larger than that affected by their light. In fact, our imaging results dovetail with those obtained spectroscopically by Altner & Matilsky (1992). Figure 3 shows M79 with one of their *IUE* aperture

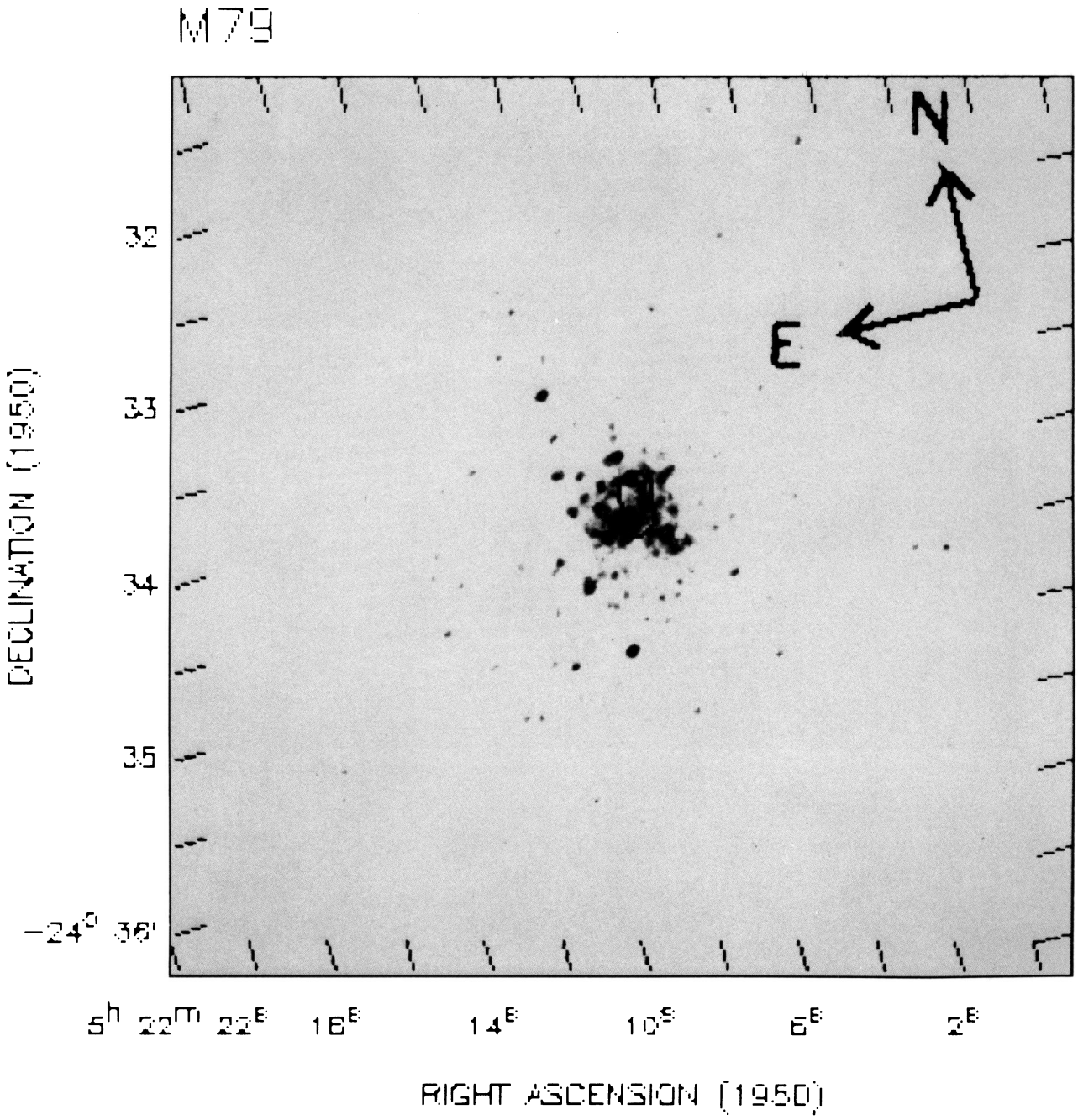

FIG. 3.—A 372 B5 exposure of M79 with an *IUE* aperture mask placed at one of the positions detailed in Altner and Matilsky (1992)

SMITH et al. (see 418, 852)

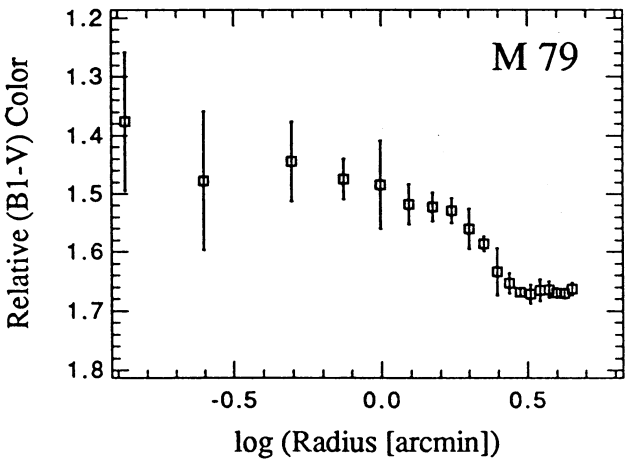

FIG. 4.—Relative ($B1 - V$) profile for the inner 4′ of M79. Errors estimated as described in the caption to Fig. 1.

positions overlaid. Within the *IUE* aperture, there are three primary maxima. While the positions of the three peaks cannot be directly compared with their four-star model (due to imprecise knowledge of the exact *IUE* positions), the spatial arrangement is in qualitative agreement. Furthermore, they find that M79 possesses an excess of UV-bright objects, consistent with our determination that it is the "bluest" globular in our sample (see Table 1 and notes to table).

3.3. *M3 (NGC 5272)*

M3 was imaged with UIT through the A5 and B5 filters. Both the near-UV and far-UV profiles for M3 are well fitted by a King model whose parameters are similar to those derived from ground-based data for the $r < 1'$. Laget et al. (1992) found that the UV profile differs with a ground-based data King model, but only at $r \geq 2'$. The UIT data are too noisy beyond 2′ (the exposure was only 200 s) to allow direct comparison with Laget et al. (1992) (exposure time $\sim$3600 s).

3.4. *M13 (NGC 6205)*

A 46 s exposure in the B5 filter reveals no significant difference between the UV and ground-based *R*-band profile. We find no significant color gradient over the range in radius ($\sim 6'' < r < 60''$), where such changes in the profiles would be reliably detectable. Cluster crowding and the UIT PSF preclude the detection of small color gradients interior to the core radius.

4. SUMMARY

4.1. *Integrated Properties*

Table 1 presents the integrated properties for the four globular clusters (plus NGC 1851, also observed by UIT and discussed in detail by Parise et al. 1993). The estimated total magnitude was obtained by integrating the intensity out to a radius beyond which no stars were seen in the UIT images. Except for NGC 1851, UV-bright stars were removed when computing these magnitudes. The "total magnitude" of ω Cen, however, is necessarily an underestimate, since the whole cluster was not imaged. We used the King model profile to estimate the total magnitude (resulting in an addition of ~ -0.1 mag). Table 1 also contains other cluster data from Webbink (1985). Without exception, the core radii in the UV are consistent with those measured from the visible.

4.2. *Helium Abundances*

Using the *R*-method (Buzzoni et al. 1983; Iben 1968), we employ our UV star counts to estimate the mean He abundance in M79. From a (*C-M*) diagram constructed with the *ground-based* data, we find 75 RGB stars exterior to $r \sim 102''$, the radius at which crowding becomes significant. Since the major contributors to the light at *B* and *V* wavelengths are the RGB stars, we scaled the number outside the $r = 102''$ radius to the *V* profile to obtain an estimate for the total number of RGB stars in M79, $\mathcal{N}_{RG} = 174 \pm 12$. Hill et al. (1992) estimated the number of HB stars in M79. Using their numbers and the relation between $\mathcal{N}_{HB}/\mathcal{N}_{RG}$ and the helium abundance *Y* [namely, $Y = 0.380 \log (\mathcal{N}_{HB}/\mathcal{N}_{RG}) + 0.176$] from Buzzoni et al. (1983), we find $Y = 0.21 \pm 0.04$. This value is slightly lower than, but consistent with, a recent helium abundance measurement by Ferraro et al. (1992) obtained solely from ground-based *B* and *V* data. The data quality for M3 and M13 prevent us from estimating the He abundance more precisely than earlier estimates using ground-based data. We hope to obtain longer exposures on these targets with the UIT during the Astro-2 mission. The detailed *C-M* diagram of ω Cen is discussed further by Whitney et al. (1993).

TABLE 1

GLOBULAR DATA

Object (1)		Total UV Flux (ergs s^{-1} cm^{-2} Å^{-1}) (2)	$E(B-V)$ (3)	Extinction (corrected mag) (4)	(far-uv–near-uv) (5)	(far-uv–V) (6)	r_c (7)	Aperture (8)
ω Cen	(B5).....	1.32 E−11	0.11	5.21	...	1.57	4.′3	27.′2
M79	(A1).....	6.01 E−13	0.01	9.37	0.42	1.94	0.17	13.3
	(B1).....	4.09 E−13	0.01	9.79	...	...	...	...
M13	(A5).....	9.55 E−12	0.02	6.29	1.74	2.10	0.95	8.9
	(B5).....	1.92 E−12	0.02	8.03	...	...	...	...
M3	(A5).....	4.25 E−12	0.01	7.25	2.81	4.03	0.48	8.9
	(B5).....	3.20 E−13	0.01	10.06	...	...	...	
NGC 1851	(A1).....	8.63 E−13	0.02	8.90	0.05	1.82	...	11.4
	(B1).....	8.23 E−13	0.02	8.95	...	...	...	...

NOTE.—Col. (1) lists the cluster name and UIT filter of the observations used here. NGC 1851 is discussed by Parise et al. 1993 and is included here for completeness. Col. (2) gives the measured UIT flux, uncorrected for reddening, with UV-bright stars removed, except in the case of NGC 1851. The apertures used for these "total" fluxes, with the exception of ω Cen, encompass the entire cluster as imaged by the UIT. Extinction corrections from col. (3) and the reddening law of Cardelli, Clayton, & Mathis 1989 were used to compute the UV magnitudes in col. (4). The colors are listed in cols (5) and (6), with *V* magnitudes coming from our ground-based data or scaled from published values. Best-fit core radii are listed in col. (7). The aperture size used for the photometry is given in col. (8).

4,3. *Profile Shapes*

We find King models to be reasonable approximations to the distribution of UV light for the four globular clusters, with this caveat: the model fits are increasingly poorer near the cluster center where the influence of discrete star clumps is high. Our ultraviolet spatial resolution ($\sim 4''$) is insufficient to detect any small-scale cusps in the stellar distribution in M13 or M3. The profile of ω Cen does show a small central cusp, possibly reflecting a statistical fluctuation of the local density. However, in the case of M79 we find significant departures of the profile shape from King models for the inner regions. We detect a significant color gradient in M79 only. Post–core collapse clusters are known to have similar color gradients (e.g., Stetson 1991), but the detection of one in M79, whose age is less than its collapse time, is interesting.

The recent detection of color gradients in several globular clusters is exciting and was interpreted as evidence for mass segregation, stellar interactions, or presence of "UV bright stars" (Djorgovski, Piotto, & King 1989; Bailyn 1989; Altner & Matilsky 1992). For three clusters observed by UIT whose ages are much less than their collapse times (M3, M13, and ω Cen) we find no evidence for a statistically significant color gradient. The color gradient observed in M79 is the product of a concentration of UV bright objects at small radii (Hill et al. 1992; Altner & Matilsky 1992) and a cluster-wide increase in the ratio of UV light to visible wavelength light with decreasing radius. This color gradient may indicate that core collapse has begun in M79 or, alternatively, that the processes which produce color gradients may set in before the cluster undergoes its core collapse. Additional *HST* high-resolution UV observations (see Guhathakurta et al. 1992), which enable the construction of cluster core color-magnitude diagrams, and UV spectroscopy are needed to pursue questions about color gradients and $\mathcal{N}_{HB}/\mathcal{N}_{RG}$ variations near the cluster centers.

We thank the whole staff of the Astro-1 mission. E. P. S. thanks S. Djorgovski for sample code of his mirror-autocorrelation technique and A. Sweigart for many useful discussions. This research was supported in part by NASA grants NAG 5-700 and NAGW-2596 to the University of Virginia.

REFERENCES

Altner, B., & Matilsky, T. A. 1992, ApJ, 410, 116
Aurière, M., & Leroy, J. L. 1990, A&A, 234, 164
Bailyn, C. D. 1989, in Dynamics of Dense Stellar Systems, ed. D. Merritt (New York: Cambridge Univ. Press), 167
Bailyn, C. D., Grindlay, J. E., Cohn, H., Lugger, P. M., Stetson, P. B., & Hesser, J. E. 1989, AJ, 98, 882
Bailyn, C. D., Sarajedini, A., Cohn, H., Lugger, P. M., & Grindley, J. E. 1992, AJ, 103, 1564
Bijaoui, A. B. 1971, A&A, 13, 232
Buzzoni, A., Fusi Pecci, F., Buonano, R., & Corsi, C. E. 1983, A&A, 128, 94
Cardelli, J., Clayton, J., & Mathis, J. S. 1989, ApJ, 345, 245
Cederblom, S. E., Moss, M. J., Cohn, H., Lugger, P. M., Bailyn, C. D., Grindlay, J. E., & McClure, R. D. 1992, AJ, 103, 480
Djorgovski, S. G. 1987, in IAU Symp. 126, Globular Cluster Systems in Galaxies, ed. J. E. Grindlay & A. G. Davis Philip (Dordrecht: Kluwer), 333
Djorgovski, S. G., Piotto, G., & King, I. R. 1989, in Dynamics of Dense Stellar Systems, ed. D. Merritt (New York: Cambridge Univ. Press), 147
Djorgovski, S. G., et al. 1991, ApJ, 372, L41
Ferraro, F. R., Clementini, G., Fusi Pecci, F., Sortino, R., & Buonanno, R. 1992, MNRAS, 256, 391
Guhathakurta, P., Yanny, B., Schneider, D. P., & Bahcall, J. N. 1992, AJ, 104, 1790
Hertz, P., & Grindlay, J. E. 1985, ApJ, 298, 95
Hill, R. S., et al. 1992, ApJ, 395, L17
Iben, I. 1968, Nature, 220, 143
King, I. R. 1962, AJ, 67, 471
———. 1966, AJ, 71, 64
Laget, M., Burgarella, D., Milliard, B., & Donas, J. 1992, A&A, 259, 510
Landsman, W. B., et al. 1992, ApJ, 395, L21
Meylan, G. 1987, A&A, 184, 144
Parise, R. A., et al. 1993, ApJ, submitted
Scaria, K. K., & Bappu, M. K. V. 1981, J. Astrophys. Astron., 2, 215
Stecher, T. P., et al. 1992, ApJ, 395, L1
Stetson, P. 1991 in Precision Photometry: Astrophysics of the Galaxy, ed. A. G. Davis-Philips, A. R. Upgren, & K. Janes (Schenectady: Davis), 69
Webbink, R. F. 1985 in IAU Symp. 113, Dynamics of Star Clusters, ed. J. Goodman & P. Hut, (Dordrecht-Kluwer), 541
Whitney, J. 1993, in preparation